Accepted Manuscript

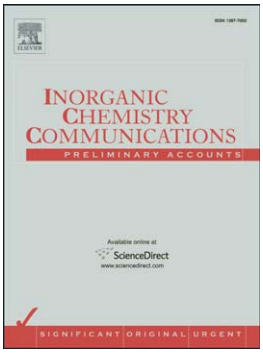

Synthesis, characterization and urease inhibition of a novel acetylhydroxamate-coordinated oxovanadium(V) complex with hydrazone ligand

Yang Huo, Yu-Ting Ye, Xiao-Shan Cheng, Zhong-Lu You

PII: S1387-7003(14)00170-1
DOI: doi: 10.1016/j.inoche.2014.04.008
Reference: INOCHE 5547

To appear in: *Inorganic Chemistry Communications*

Received date: 12 January 2014
Revised date: 8 April 2014
Accepted date: 10 April 2014

Please cite this article as: Yang Huo, Yu-Ting Ye, Xiao-Shan Cheng, Zhong-Lu You, Synthesis, characterization and urease inhibition of a novel acetylhydroxamate-coordinated oxovanadium(V) complex with hydrazone ligand, *Inorganic Chemistry Communications* (2014), doi: 10.1016/j.inoche.2014.04.008

This is a PDF file of an unedited manuscript that has been accepted for publication. As a service to our customers we are providing this early version of the manuscript. The manuscript will undergo copyediting, typesetting, and review of the resulting proof before it is published in its final form. Please note that during the production process errors may be discovered which could affect the content, and all legal disclaimers that apply to the journal pertain.

ACCEPTED MANUSCRIPT

Synthesis, characterization and urease inhibition of a novel acetylhydroxamate-coordinated oxovanadium(V) complex with hydrazone ligand

Yang Huo[a], Yu-Ting Ye[a], Xiao-Shan Cheng[a], Zhong-Lu You[a,b,*]

[a] Department of Chemistry and Chemical Engineering, Liaoning Normal University, Dalian 116029, P. R. China

[b] State Key Laboratory of Coordination Chemistry, Nanjing University, Nanjing 210093, P.R. China

Abstract

The first example of a novel acetylhydroxamate-coordinated oxovanadium(V) complex with hydrazone ligand has been prepared and structurally characterized. The urease inhibitory activity of the complex was assayed, and the molecular docking study was performed. The complex has strong urease inhibitory activity. The introduction of acetylhydroxamate ligand as functional urease inhibitory group may increase the activity of the complex.

Keywords: Hydrazone; Acetylhydroxamate; Oxovanadium complex; Crystal structure; Urease inhibition

Urease is a nickel-containing metalloenzyme that catalyzes the hydrolysis of urea to form ammonia and carbamate [1,2]. The resulting carbamate spontaneously decomposes to yield a second molecule of ammonia and carbon dioxide. High concentration of ammonia arising from the reaction, as well as the accompanying pH elevation, has important negative implications in medicine and agriculture [3–5]. Control of the activity of urease through the use of inhibitors could counteract these negative effects. In recent years, urease inhibitors play an important role in the treatment of the infections caused by urease producing bacteria [6]. Inhibitors of urease can be broadly classified into two species: (1) organic compounds, such as acetohydroxamic acid, humic acid, and 1,4-benzoquinone [7–8]; (2) heavy metal ions, such as Cu^{2+}, Zn^{2+}, Pd^{2+}, and Cd^{2+} [10,11]. Considering the metal complexes are a kind

* Corresponding author.
E-mail address: youzhonglu@lnnu.edu.cn (Zhong-Lu You).

ACCEPTED MANUSCRIPT

of versatile enzyme inhibitors [12], we have recently reported the urease inhibitory activities of a number of complexes with Schiff bases [13-15]. The results show that some Schiff base copper(II) complexes have potential urease inhibitory activities. Vanadium complexes have been widely investigated in biological chemistry, especially for their insulin-enhancing activities [16-18]. During the search of literature, we found that vanadium(IV) complexes bearing hydrazone ligands also possess interesting urease inhibitory activities [19]. Acetylhdroxamic acid (AHA) is a commercial urease inhibitor. The obvious short-coming of this substance is that it is very soluble in water and readily to lose from soil. From the point of coordination chemistry, AHA is also a potential bidentate ligand. Can the binding of AHA to oxovanadium complex with hydrazone ligand bearing effective urease inhibition? If yes, it can not only increase the utilization rate of AHA, but also form more complicated urease inhibitors. Based on this consideration, in this paper, a novel acetylhdroxamate (AH) coordinated oxovanadium(V) complex, $[VO_2L(AH)]$ (H_2L = *N′*-(5-bromo-2-hydroxybenzylidene)-3-nitrobenzohydrazide; Scheme 1), was synthesized and structurally characterized. The urease inhibitory activity of the complex was investigated from both experimental and molecular docking analysis [20].

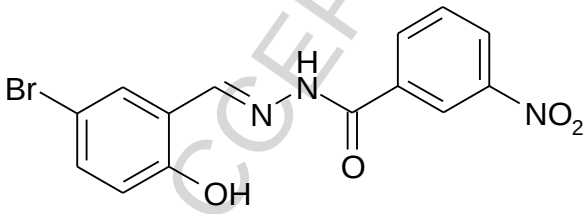

Scheme 1. H_2L.

The yellow crystalline product of the hydrazone ligand H_2L was prepared by reaction of equimolar quantities of 5-bromosalicylaldehyde with 3-nitrobenzohydrazide in ethanol and subsequent evaporation of the solvent. Yield: 91%. Anal. Calc. for $C_{14}H_{10}BrN_3O_4$: C 46.2, H 2.8, N 11.5%. Found: C 46.0, H 2.8, N 11.6%. Selected IR data (KBr, cm^{-1}): ν 1617 (s, C=N).

An ethanolic solution (20 mL) of H_2L (0.5 mmol, 0.182 g) and AHA (0.5 mmol, 0.038 g) mixed together was added with stirring to an ethanolic solution (20 mL) of $VO(acac)_2$ (0.5 mmol, 0.133 g). The mixture was stirred at room temperature for 30 min to give deep brown solution. Brown block-shaped single crystals suitable for X-ray diffraction were formed by slow evaporation of the solution in air for a few days.

ACCEPTED MANUSCRIPT

Yield: 68%. Anal. Calc. for $C_{18}H_{18}BrN_4O_8V$: C 39.4, H 3.3, N 10.2%. Found: C 39.3, H 3.4, N 10.1%. Selected IR data (KBr, cm^{-1}): 3435 (br, m, O–H), 1603 (s, C=N), 969 (m, V=O).

Diffraction intensities for the complex were collected at 298(2) K using a Bruker SMART CCD detector with Mo-Kα radiation (λ = 0.71073 Å). The collected data were reduced using SAINT program [21], and multi-scan absorption corrections were performed using SADABS program [22]. The structure was solved by direct method and refined against F^2 by full-matrix least-squares method using SHELXTL [23]. All non-hydrogen atoms were refined anisotropically. The amino H was located from a difference Fourier map and refined isotropically, with N–H distance restrained to 0.90(1) Å. The remaining hydrogen atoms were placed in calculated positions and constrained to ride on their parent atoms.

The measurement of *Helicobacter pylori* urease inhibitory activity was carried out for three parallel times. *Helicobacter pylori* (ATCC 43504; American Type Culture Collection, Manassas, VA) was grown in brucella broth supplemented with 10% heat-inactivated horse serum for 24 h at 37 ºC under microaerobic conditions (5% O_2, 10% CO_2, and 85% N_2). The method of preparation of *Helicobacter pylori* urease by Mao was followed [24]. Briefly, broth cultures (50 mL, 2.0×10^8 CFU mL^{-1}) were centrifuged (5000 g, 4 ºC) to collect the bacteria, and after washing twice with phosphate-buffered saline (pH = 7.4), the *Helicobacter pylori* precipitation was stored at –80 ºC. *Helicobacter pylori* was returned to room temperature, and after addition of 3 mL of distilled water and protease inhibitors, sonication was performed for 60 s. Following centrifugation (15,000 g, 4 ºC), the supernatant was desalted through SephadexG-25 column (PD-10 columns, Amersham–Pharmacia Biotech, Uppsala, Sweden). The resultant crude urease solution was added to an equal volume of glycerol and stored at 4 ºC until use in the experiment. The mixture, containing 25 μL (4U) of *Helicobacter pylori* urease and 25 μL of the test compound, was pre-incubated for 3 h at room temperature in a 96-well assay plate. Urease activity was determined by measuring ammonia production using the indophenol method as described by Weatherburn [25].

Molecular docking of the complex into the three-dimensional X-ray structures of *Helicobacter pylori urease* structure (entry 1E9Z in the Protein Data Bank) was carried out using the AUTODOCK 4.0 software as implemented through the graphical user

ACCEPTED MANUSCRIPT

interface AutoDockTools (ADT 1.4.6).

The graphical user interface AUTODOCKTOOLS was employed to setup the enzymes: all hydrogens were added, Gasteiger charges were calculated and nonpolar hydrogens were merged to carbon atoms. The Ni initial parameters are set as r = 1.170 Å, q = +2.0, and van der Waals well depth of 0.100 kcal/mol [26]. The 3D structures of ligand molecule were saved in Mol2 format with the aid of the program MERCURY. The partial charges of Mol2 file were further modified by using the ADT package (version 1.4.6) so that the charges of the nonpolar hydrogens atoms assigned to the atom to which the hydrogen is attached. The resulting file was saved as a pdbqt file.

The AUTODOCKTOOLS program was used to generate the docking input files. In the docking a grid box size of 60 × 60 × 70 points in x, y, and z directions was built, the map was centered on Ni3001 atom in the catalytic site of the protein. A grid spacing of 0.375 Å and a distances-dependent function of the dielectric constant were used for the calculation of the energetic map. 100 runs were generated by using Lamarckian genetic algorithm searches. Default settings were used with an initial population of 50 randomly placed individuals, a maximum number of 2.5×10^6 energy evaluations, and a maximum number of 2.7×10^4 generations. A mutation rate of 0.02 and a crossover rate of 0.8 were chosen. The results of the most favorable free energy of binding were selected as the resultant complex structure.

The hydrazone ligand H_2L and the oxovanadium(V) complex were readily prepared at room temperature. The molar conductance value of the complex measured in acetonitrile at concentration of 10^{-3} M is 27 Ω^{-1} cm^2 mol^{-1}, indicating the non-electrolytic nature of the complex [27].

The hydrazone ligand has stretching bands attributed to C=O, C=N, C–OH and NH at 1651, 1617, 1153 and 1236, and 3251 cm^{-1}, respectively. The complex exhibits typical bands at 969 cm^{-1}, which is assigned to the V=O vibration [28]. The band due to $\nu_{C=O}$ was absent in the complex, and new C–O stretch appeared at 1272 cm^{-1}. This suggests occurrence of *keto*-imine tautomerization of the ligand during complexation. The $\nu_{C=N}$ absorption observed at 1617 cm^{-1} in the free hydrazone ligand shifted to 1603 cm^{-1} for the complex upon coordination to the V atom. The weak peaks in the low wave numbers at 490 and 586 cm^{-1} may be attributed to V–O and V–N bonds in the

ACCEPTED MANUSCRIPT

complex.

The molecular structure of the complex is shown in Figure 1. X-ray crystallography [29] reveals that the asymmetric unit of the complex contains a mononuclear oxovanadium(V) species and an ethanol molecule. The coordination geometry around the V atom is highly distorted octahedral. The hydrazone ligand behaves in a tridentate manner in which the phenolate O, imino N, and enolate O atoms occupy a meridional plane. The acetylhydroxamate ligand behaves in a bidentate manner, and coordinates to the V atom through the deprotonated hydroxyl O atom and the carbonyl O atom. The equatorial plane of the octahedral coordination is defined by O1, N1, O2 and O6 atoms, and the axial positions are occupied by O2 and O7 atoms. The distortion of the octahedral geometry can be evidenced by the coordinate bond lengths and angles. The V1–O5 bond is significantly longer than the other V–O bonds, yet, it is not uncommon for such complexes [30-32]. The equitorial atoms show high degree of planarity, with mean deviation from plane of 0.020(3) Å. The V atom deviates from the least-squares plane defined by the four equitorial atoms by 0.290(1) Å. All the bond lengths in the complex are comparable to those observed in similar vanadium(V) complexes [30-32]. The angular distortion in the octahedral environment around V comes from the five- and six-membered chelate rings taken by the hydrazone ligand. For the same reason, the *trans* angle significantly deviates from the ideal value of 180°. The hydrazone ligand in is approximately planar, with the dihedral angle between the two benzene rings of 3.8(3)°.

In the crystal structure of the complex, mononuclear oxovanadium complex molecules are linked by ethanol molecules through intermolecular N4–H4···O8 and O8–H8···O5^{i} hydrogen bonds [N4–H4 = 0.90(1) Å, H4···O8 = 1.823(6) Å, N4···O8 = 2.716(3) Å, N4–H4···O8 = 172°; O8–H8 = 0.82 Å, H8···O5^{i} = 2.076(7) Å, O8···O5^{i} = 2.862(3) Å, O8–H8···O5^{i} = 161°; symmetry code for i: x – 1, y, z], to form 1D chains running down the *a*-axis direction (Figure 2). In addition, there are weak π···π interactions among the benzene rings of the hydrazone ligand and the V1-O2-C8-N2-N1 and V1-O5-C16-N4-O6 chelate rings.

[Insert Figures 1 and 2 about here]

Differential thermal (DT) and thermal gravimetric analyses (TGA) were conducted to examine the stability of the complex (Figure 3). There are four steps of decomposition. The first step started at 140 °C and ended at 159 °C, with a weight loss of 8.5%, which is caused by the loss of the ethanol molecule (8.4%). Actually, the

ACCEPTED MANUSCRIPT

complex was first decomposed at 160 °C and completed at 490 °C. It is difficult to ascribe the remaining three steps of decomposition. The weight loss of these three steps is 77%, corresponding to the loss of the hydrazone and acetylhdroxamate ligands and the formation of V_2O_5. The total weight loss of 85.5% is close to the idea value of 84.3%.

[Insert Figure 3 about here]

The percentage inhibition at concentration of 100 μM for the complex is 96.2 ± 4.5. The acetohydroxamic acid was used as a reference [6] with percentage of inhibition of 87.3 ± 3.3. The IC_{50} value of 8.3 ± 1.6 μM for the complex is superior to that of AHA (37.2 ± 1.7 μM), and also stronger than that of vanadyl sulfate (196 ± 7 μM) and the vanadium complexes we reported previously [30, 33]. As a detailed comparison, the hydrazone ligand itself has no activity at the concentration of 100 μM. The vanadium complex formed by the reaction of the hydrazone ligand and $VO(acac)_2$ without the addition of AHA has effective urease inhibition (100 μM, 72%; IC_{50} = 21.5 μM), yet, it is obvious weaker than the complex reported herein. Lineweaver-Burk plots of 1/absorbance versus 1/urea were used to determine the type of enzyme inhibition (Figure 4). The plots show that the complex inhibits the urease in a mixed mode.

[Insert Figure 4 about here]

The enzyme surface model and the weak interactions of the complex with the enzyme are shown in Figures 5 and 6, respectively. It is obvious that the complex molecule is well filled in the active pocket of the urease, with the nitrobenzene and acetylhydroxamate segments inserted in the hole. The nitro group of the ligand is much close to the two Ni atoms of the active center of the urease. The complex forms weak interactions with ASP165, ASN168, HIS138, KCX219, ASP362, ALA365, GLY279, MET366, ARG338 and CYS321 of the urease. As a result, the docking score (–12.8) of the complex is much lower than that of AHA (–5.0).

[Insert Figures 5 and 6 about here]

Conclusion

In summary, the present paper reports the first example of a novel acetylhydroxamate coordinated oxovanadium(V) complex with *N'*-(5-bromo-2-hydroxybenzylidene)-3-nitrobenzohydrazide. The complex show strong urease inhibitory activity, with IC_{50} value of 8.3 ± 1.6 μM. The complex may be used in the treatment of infections caused by urease producing bacteria, which deserves further study.

ACCEPTED MANUSCRIPT

Acknowledgement

This work was financially supported by the Natural Science Foundation of China (Project No. 20901036).

References

[1] P.A. Karplus, M.A. Pearson, R.P. Hausinger, 70 years of crystalline urease: What have we learned? Acc. Chem. Res. 30 (1997) 330–337.

[2] J.B. Sumner, The isolation and crystallization of the enzyme urease, J. Biol. Chem. 69 (1926) 435–441.

[3] L.E. Zonia, N.E. Stebbins, J.C. Polacco, Essential role of urease in germination of nitrogen-limited arabidopsis-thaliana seeds, Plant Physiol. 107 (1995) 1097–1103.

[4] C.M. Collins, S.E.F. DÓrazio, Bacterial ureases – structure, regulation of expression and role in pathogenesis, Mol. Microbiol. 9 (1993) 907–913.

[5] C. Montecucco, R. Rappuoli, Living dangerously: How Helicobacter pylori survives in the human stomach, Nat. Rev. Mol. Cell Biol. 2 (2001) 457–466.

[6] B. Krajewska, Ureases I. Functional, catalytic and kinetic properties: A review, J. Mol. Catal. B. Enzym. 59 (2009) 9–21.

[7] Z. Amtul, Atta-ur-Rahman, R.A. Siddiqui, M.I. Choudhary, Chemistry and mechanism of urease inhibition, Curr. Med. Chem. 9 (2002) 1323–1348.

[8] W. Zaborska, M. Kot, K. Superata, Inhibition of jack bean urease by 1,4-benzoquinone and 2,5-dimethyl-1,4-benzoquinone. Evaluation of the inhibition mechanism, J. Enzym. Inhib. Med. Chem. 17 (2002) 247–253.

[9] M.A. Pearson, L.O. Michel, R.P. Hausinger, P.A. Karplus, Structures of Cys319 variants and acetohydroxamate-inhibited Klebsiella aerogenes urease, Biochemistry 36

ACCEPTED MANUSCRIPT

(1997) 8164–8172.

[10] W. Zaborska, B. Krajewska, Z. Olech, Heavy metal ions inhibition of jack bean urease: Potential for rapid contaminant probing, J. Enzym. Inhib. Med. Chem. 19 (2004) 65–69.

[11] W. Zaborska, B. Krajewska, M. Leszko, Z. Olech, Inhibition of urease by Ni^{2+} ions - Analysis of reaction progress curves, J. Mol. Catal. B: Enzym. 13 (2001) 103–108.

[12] A.Y. Louie, T.J. Meade, Metal complexes as enzyme inhibitors, Chem. Rev. 99 (1999) 2711–2734.

[13] Z.-L. You, L. Zhang, D.-H. Shi, X.-L. Wang, X.-F. Li, Y.-P. Ma, Synthesis, crystal structures and urease inhibitory activity of copper(II) complexes with Schiff bases, Inorg. Chem. Commun. 13 (2010) 996–998.

[14] Z.-L. You, L.-L. Ni, D.-H. Shi, S. Bai, Synthesis, structures, and urease inhibitory activities of three copper(II) and zinc(II) complexes with 2-{[2-(2-hydroxyethylamino)ethylimino]methyl}-4-nitrophenol, Eur. J. Med. Chem. 45 (2010) 3196–3199.

[15] P. Hou, Z.-L. You, L. Zhang, X.-L. Ma, L.-L. Ni, Synthesis, crystal structures, and urease inhibitory activities of two azido-bridged polynuclear copper(II) complexes with Schiff bases, Transition Met. Chem. 33 (2008) 1013–1017.

[16] M.J. Pereira, E. Carvalho, J.W. Eriksson, D.C. Crans, M. Aureliano, Effects of decavanadate and insulin enhancing vanadium compounds on glucose uptake in isolated rat adipocytes, J. Inorg. Biochem. 103 (2009) 1687–1692.

[17] M.-J. Xie, X.-D. Yang, W.-P. Liu, S.-P. Yan, Z.-H. Meng, Insulin-enhancing activity of a dinuclear vanadium complex: 5-chloro-salicylaldhyde ethylenediamine oxovanadium(V) and its permeability and cytotoxicity, J. Inorg. Biochem. 104 (2010) 851–857.

ACCEPTED MANUSCRIPT

[18] J.J. Smee, J.A. Epps, K. Ooms, S.E. Bolte, T. Polenova, B. Baruah, L.Q. Yang, W.J. Ding, M. Li, G.R. Willsky, A. la Cour, O.P. Anderson, D.C. Crans, Chloro-substituted dipicolinate vanadium complexes: Synthesis, solution, solid-state, and insulin-enhancing properties, J. Inorg. Biochem. 103 (2009) 575–584.

[19] R. Ara, U. Ashiq, M. Mahroof-Tahir, Z.T. Maqsood, K.M. Khan, M.A. Lodhi, M.I. Choudhary, Chemistry, urease inhibition, and phytotoxic studies of binuclear vanadium(IV) complexes, Chem. Biodivers. 4 (2007) 58–71.

[20] R. Huey, G.M. Morris, A.J. Olson, D.S. Goodsell, A semiempirical free energy force field with charge-based desolvation, J. Comput. Chem. 28 (2007) 1145–1152.

[21] Bruker, SMART and SAINT. Bruker AXS Inc, Madison (2002).

[22] G.M. Sheldrick, SADABS. University of Göttingen, Germany (1996).

[23] G.M. Sheldrick, SHELXTL V5.1, Software Reference Manual, Bruker AXS Inc, Madison (1997).

[24] W.J. Mao, P.C. Lv, L. Shi, H.Q. Li, H.L. Zhu, Synthesis, molecular docking and biological evaluation of metronidazole derivatives as potent *Helicobacter pylori urease* inhibitors, Bioorg. Med. Chem. 17 (2009) 7531–7536.

[25] M.W. Weatherburn, Phenol-hypochlorite reaction for determination of ammonia, Anal. Chem. 39 (1967) 971–974.

[26] B. Krajewska, W. Zaborska, Jack bean urease: The effect of active-site binding inhibitors on the reactivity of enzyme thiol groups, Bioorg. Chem. 35 (2007) 355–365.

[27] W.J. Geary, The use of conductivity measurements in organic solvents for the characterisation of coordination compounds, Coord. Chem. Rev. 7 (1971) 81–122.

[28] A. Sarkar, S. Pal. Some ternary complexes of oxovanadium(IV) with

ACCEPTED MANUSCRIPT

acetylacetone and *N*-(2-pyridyl)-*N'*-(salicylidene)hydrazine and its derivatives. Polyhedron 25 (2006) 1689–1694.

[29] The crystal data and structural parameters for the complex: $C_{18}H_{18}BrN_4O_8V$, M = 549.2, triclinic, space group P-1, a = 7.2101(8) Å, b = 8.6546(9) Å, c = 17.604(2) Å, α = 92.873(3)°, β = 91.677(3)°, γ = 97.991(3)°, V = 1085.8(2) Å^3, Z = 2, ρ_{calcd} = 1.680 g cm^{-3}, T = 298(2) K, μ(Mo Kα) = 2.350 mm^{-1}, R_1 = 0.0467, wR_2 = 0.1146.

[30] Z.-L. You, D.-H. Shi, J.-C. Zhang, Y.-P. Ma, C. Wang, K. Li. Synthesis, structures, and urease inhibitory activities of oxovanadium(V) complexes with Schiff bases. Inorg. Chim. Acta 384 (2012) 54–61.

[31] H.H. Monfared, S. Alavi, R. Bikas, M. Vahedpour, P. Mayer. Vanadiumoxo-aroylhydrazone complexes: Synthesis, structure and DFT calculations. Polyhedron 29 (2010) 3355-3362.

[32] M.R. Maurya, S. Agarwal, C. Bader, M. Ebel, D. Rehder. Synthesis, characterization and catalytic potential of hydrazonato-vanadium(V) model complexes with $[VO]^{3+}$ and $[VO_2]^+$ cores. Dalton Trans. (2005) 537–544.

[33] Y. Zhao, X. Han, X.-X. Zhou, H.-H. Li, Z.-L. You. Synthesis, structures, and helicobacter pylori urease inhibition of oxovanadium(V) complexes with hydrazones. Chinese J. Inorg. Chem. 29 (2013) 867–874.

ACCEPTED MANUSCRIPT

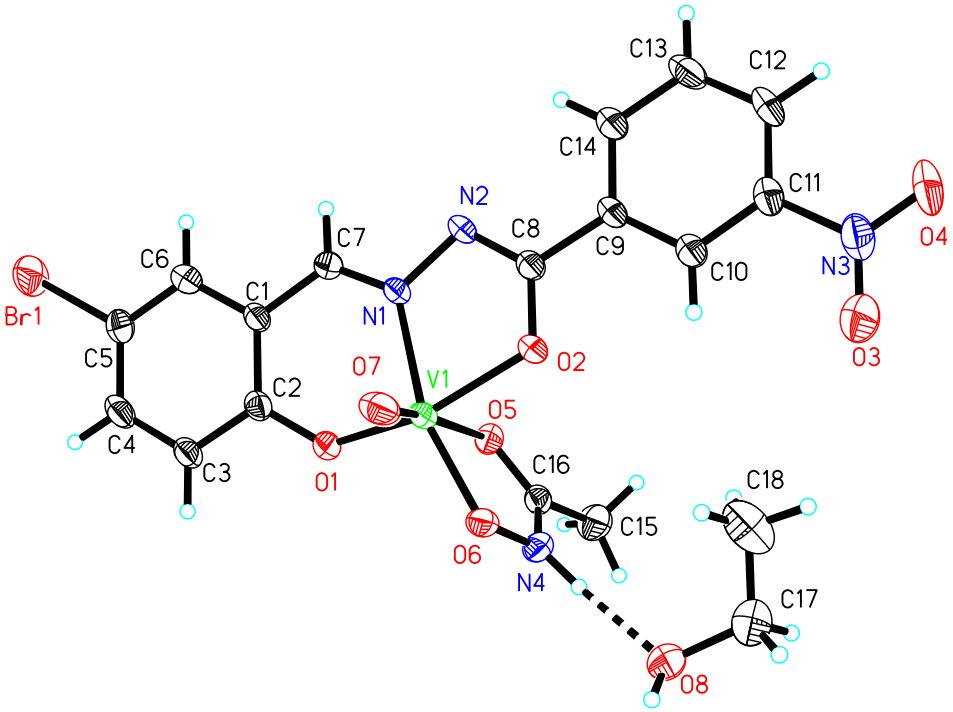

Figure 1. A perspective view of the molecular structure of the complex with the atom labeling scheme. Thermal ellipsoids are drawn at the 30% probability level. Selected bond lengths (Å) and bond angles (°): V1-O1 1.854(3), V1-O2 1.950(2), V1-O5 2.235(2), V1-O6 1.856(2), V1-O7 1.583(3), V1-N1 2.085(3); O7-V1-O1 100.2(1), O7-V1-O6 96.5(1), O1-V1-O6 104.2(1), O7-V1-O2 99.2(1), O1-V1-O2 153.7(1), O6-V1-O2 91.0(1), O7-V1-N1 99.2(1), O1-V1-N1 84.4(1), O6-V1-N1 160.4(1), O2-V1-N1 75.1(1), O7-V1-O5 172.2(1), O1-V1-O5 83.3(1), O6-V1-O5 75.8(1), O2-V1-O5 79.8(1), N1-V1-O5 88.1(1).

ACCEPTED MANUSCRIPT

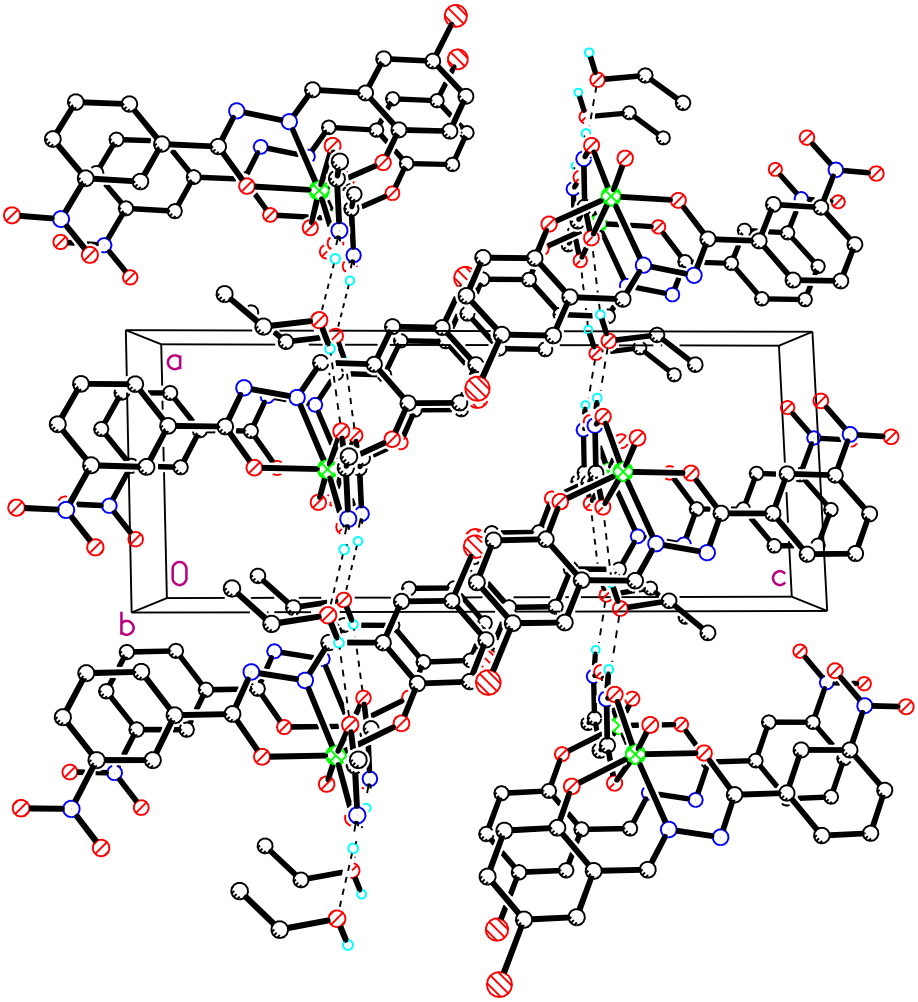

Figure 2. Molecular packing diagram of the complex, viewed along the axis-*b* direction. Hydrogen bonds are shown as dashed lines.

ACCEPTED MANUSCRIPT

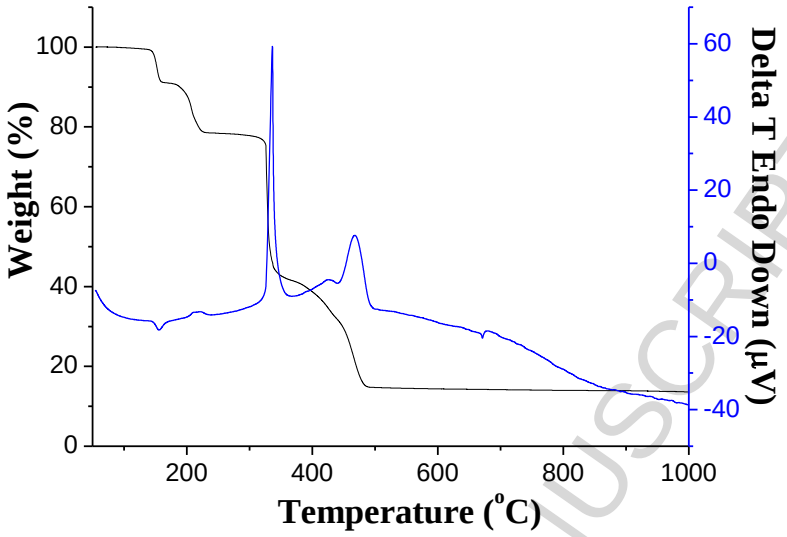

Figure 3. DT-TGA curve of the complex.

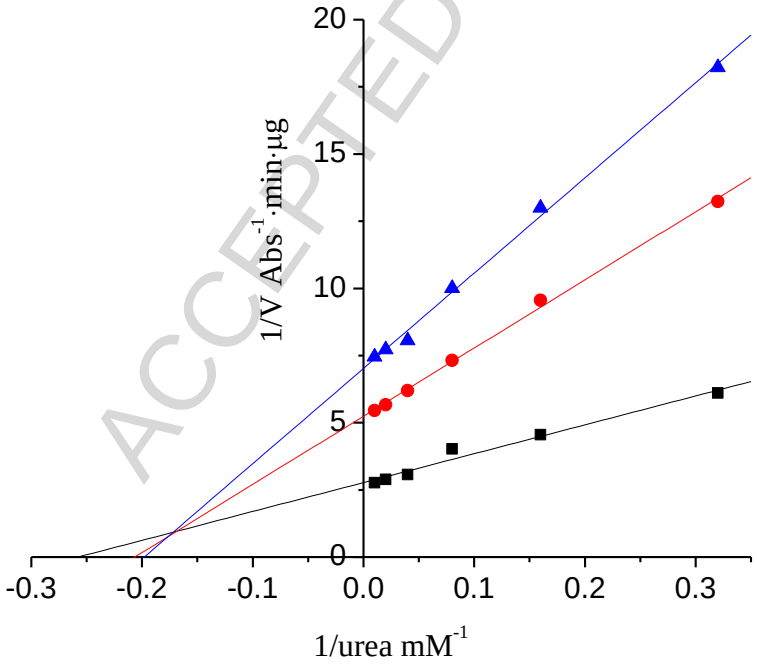

Figure 4. Lineweaver–Burk plot of inhibition of urease by the complex. ■ no complex present. The straight line plots refer to the complex concentrations of 5.50 µg·mL^{-1} (●) and 11.00 µg·mL^{-1} (▲).

ACCEPTED MANUSCRIPT

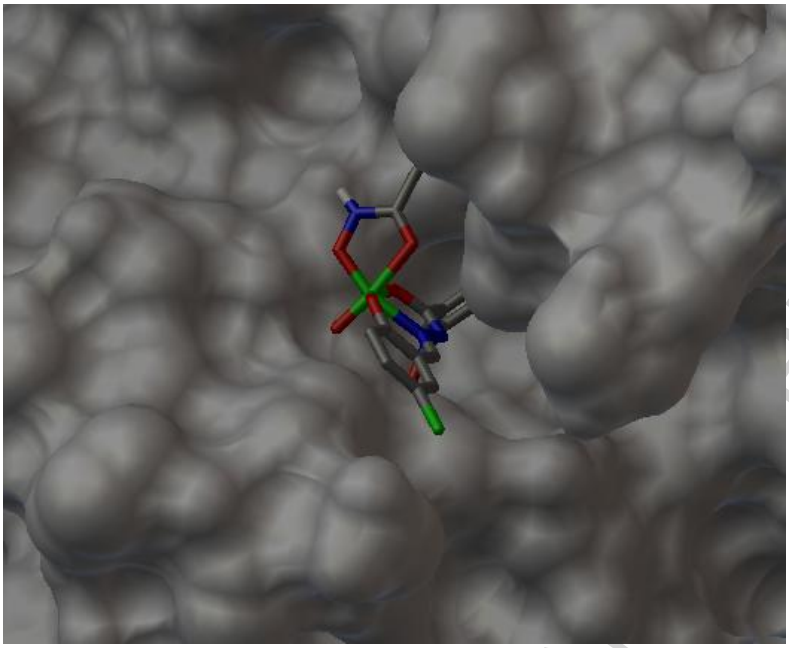

Figure 5. The receptor surface model of the complex for *Helicobacter pylori* urease. The enzyme is shown as Surface. The complex is shown as sticks.

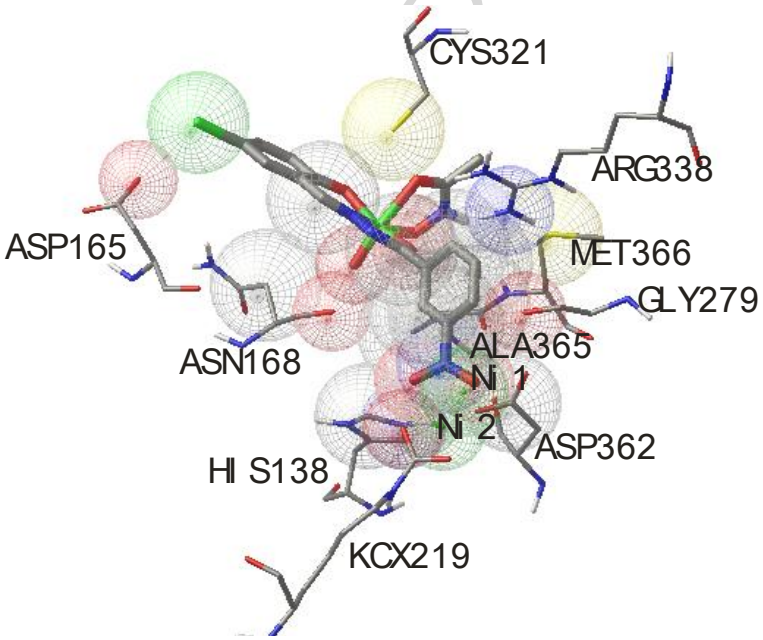

Figure 6. Binding model of the complex with the active site of *Helicobacter pylori* urease. Weak interactions are shown as dashed lines.

ACCEPTED MANUSCRIPT

Graphical Abstract

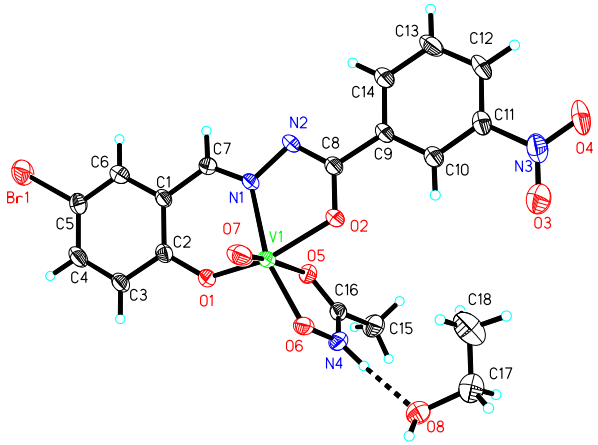

The first example of a novel acetylhydroxamate coordinated oxovanadium(V) complex with hydrazone ligand was obtained. The complex show strong urease inhibitory activity with IC_{50} value of 8.3 ± 1.6 μM.

ACCEPTED MANUSCRIPT

Highlights

► A novel acetylhydroxamate coordinated oxovanadium(V) complex was prepared. ► The complex has been characterized by single crystal X-ray diffraction. ► Thermal stability was studied. ► The complex show strong urease inhibitory activity.

ACCEPTED MANUSCRIPT